

Avoiding unphysical kinetic traps in Monte Carlo simulations of strongly attractive particles

Stephen Whitelam and Phillip L. Geissler

*Department of Chemistry, University of California at Berkeley,
and Physical Biosciences and Materials Sciences Divisions,
Lawrence Berkeley National Laboratory, Berkeley, CA 94720*

(Dated: December 2, 2024)

We introduce a ‘virtual-move’ Monte Carlo (VMMC) algorithm for systems of pairwise-interacting particles. This algorithm permits the realistic evolution of particles possessing attractions of arbitrary strength, range and geometry, an important realization being self-assembling particles endowed with strong, short-ranged and angularly specific (‘patchy’) attractions. Molecular dynamics simulations accomplish a realistic evolution of such systems by updating simultaneously the position of every particle. Standard Monte Carlo techniques, however, employ sequential updates of particles, and suffer from low acceptance rates when attractions are strong. Our algorithm, which satisfies detailed balance, avoids this slowing-down by proposing simultaneous moves of collections (clusters) of particles. Neighbouring particle pairs first execute virtual ‘trial’ moves. By calculating bond energies before and after these virtual moves, we determine whether to move these particles collectively or individually. We iterate this scheme over all particle pairs, and update simultaneously the positions of all particles. Barring particle overlaps this scheme is rejection-free, and it evolves particles in a physical manner without the need for the explicit computation of forces required by molecular dynamics simulations. We discuss the virtual-move algorithm in the context of other Monte Carlo cluster-move schemes, and demonstrate its utility by applying it to a model of biological self-assembly.

PACS numbers: 02.70.Tt, 87.53.Wz

I. INTRODUCTION

A standard Monte Carlo simulation of a system of particles consists of a sequence of moves of *individual* particles. If these moves are proposed and accepted so as to ensure detailed balance (or the weaker condition of balance [1, 2]), the system will eventually relax to thermal equilibrium [3]. This approach even provides an approximation to the dynamics that the corresponding physical system might execute [4, 5, 6]. However, equilibration can become very slow when relaxation requires the movement of particles in concert, particularly in the presence of very strong interactions. This is the case, for example, when small ions of opposite charge bind together tightly.

In Figure 1 we show a simple situation in which a standard Monte Carlo simulation suffers a dramatic slowing-down in the presence of a very strong, short-ranged attraction. We consider four particles, endowed with short-ranged pair interactions, with only two (1 and 2) close enough to interact. For this system to relax, the strongly-bound dimer 12 must move until it collides with either free particle. Molecular dynamics simulations accomplish this collective movement by updating *simultaneously* the position of every particle: if 1 or 2 moves, the force on the other is calculated and the positions of both corrected, ensuring that the dimer remains intact. A standard Monte Carlo simulation, however, employs *sequential* updates of individual particle positions. Any move (e.g. $\mathbf{a} \rightarrow \mathbf{b}$) of particle 1 or 2 which breaks the 12 interaction is suppressed by the exponential of the dimer binding energy. If this energy is but a few multiples of

$k_B T$, such a break is almost never accepted. In order for the dimer 12 to move substantially, the single-particle move must be so small that it does not break the short-ranged bond, leading to very long relaxation times.

This problem can be overcome in principle by proposing a simultaneous move of particles 1 and 2 ($\mathbf{a} \rightarrow \mathbf{c}$), and in general moves of clusters of particles. Existing cluster algorithms [7, 8, 9] have been used with great success to simulate many complex systems [10]. Such algorithms define a cluster to be moved by recursively linking particle pairs with a given probability. In general, this probability is $p = 1 - e^{\beta\epsilon}$, which depends on the reciprocal of the Boltzmann weight associated with the pair energy $\epsilon < 0$. This choice makes efficient use of computer resources, because detailed balance dictates that moves of clusters defined in this manner are always accepted, provided that no particle overlap occurs.

However, these rejection-free algorithms encounter problems when the attraction strength $-\epsilon$ between particles becomes very large. Strongly-bonded particles are invariably assigned to the same cluster, and so are not moved relative to each other. Thus the possibility of replacing their strong bond with one even stronger is rarely tested. Such unphysical kinetic traps severely impede the exploration of dense, ordered structures, by preventing the particles comprising a cluster from exploring local gradients in potential energy. These explorations occur in many phase transitions, such as the microphase separation of colloids at low temperature, and in self-assembly, e.g. of large proteins called chaperonins [11, 12, 13]; various nanoparticles [14, 15, 16]; and virus capsids [17, 18].

In this paper we show briefly that one can restore er-

godicity to conventional cluster moves in a computationally efficient way. Particle pairs are linked with a probability depending on a pseudo-Boltzmann weight containing a fictitious temperature T_f in general greater than the true temperature. By varying this fictitious temperature we can interpolate between choosing the system's most strongly-bonded clusters, when $T_f = T$, and choosing single particles, at infinite fictitious temperature. Thus one can propose moves which test the resilience of strong, but non-optimal interactions.

However, defining clusters according to bond energies results in an unphysical dynamics (see Appendix). To resolve this problem, we can define clusters according to bond energy gradients by using a *dynamic* linking procedure. Here we introduce a cluster algorithm designed to evolve in a physical manner a collection of strongly-attractive particles, and so permit the simulation of particles that spontaneously self-assemble. Such particles typically possess pairwise attractions of arbitrary strength, possibly very short range, and a high degree of angular specificity ('patchiness'). Our algorithm is a 'virtual-move' Monte Carlo (VMMC) scheme in which neighbouring particle pairs first execute virtual trial moves. By calculating bond energies before and after these virtual moves, we determine whether to move these particles collectively or individually. We iterate this scheme over all particle pairs, and update simultaneously the positions of all particles. At this point the Monte Carlo acceptance probability is evaluated; this turns out to be unity if we accept each virtual move according to a particular probability (to be specified later).

This scheme evolves particles in a physical manner, while bypassing the need for the explicit computation of forces required by molecular dynamics simulations. Although this is in principle true of standard single-particle Monte Carlo schemes, the latter suffer a dramatic slowing-down in the presence of strong, short-ranged interactions, rendering them unsuitable for evolving typical self-assembling systems. The VMMC algorithm mimics the physical, simultaneous updates of particle positions characteristic of molecular dynamics simulations, whilst retaining the traditional advantages of the Monte Carlo approach. The latter include the ability to deal with pathological (e.g. perfectly sharp) potentials, and to employ a basic step size larger than that required by MD simulations.

This paper is organised as follows. In Section II we show how one can restore ergodicity to conventional MC cluster algorithms, and we demonstrate in Section III how this restoration helps avoid unphysical kinetic traps which plague conventional cluster algorithms when applied to strongly-interacting particles. In Sections IV and V we turn to dynamics. Although often regarded purely as a tool for obtaining equilibrium averages, a Monte Carlo simulation can in many cases closely approximate natural dynamics. In Section IV we describe the central result of this paper. We show that by proposing moves of particles based upon individual bond energy gradients,

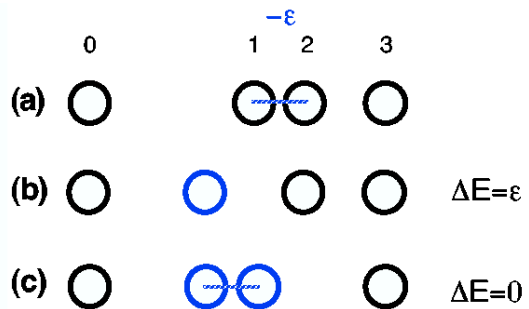


FIG. 1: An illustration of the difficulty encountered by standard Monte Carlo methods in the presence of very strong, short-ranged interactions. Here we show four particles, labeled 0,1,2 and 3, possessing pairwise interactions. Only particles 1 and 2 are close enough to interact, and they do so with energy $\epsilon_{12} = -\epsilon$ (bond shown in blue), with $\epsilon \gg k_B T$. A natural dynamics would see particles 0 and 3 diffuse individually, and particles 1 and 2 diffuse as a dimer, until a collision between these bodies took place. In a molecular dynamics simulation particle positions are updated *simultaneously*. At each stage particles 1 and 2 will move collectively. However, a standard Monte Carlo scheme involves *sequential* moves of individual particles. Any move of particle 1 which breaks the bond with particle 2 (and most meaningful moves will, because the bond is short-ranged) (a \rightarrow b) is rejected with a probability $1 - e^{-\epsilon/k_B T} \approx 1$; no significant motion of particles 1 or 2 is possible. The solution is to move particles 1 and 2 simultaneously (a \rightarrow c). We shall discuss different ways of choosing aggregates of particles to move in order to 1) restore ergodicity to conventional Monte Carlo schemes, and 2) ensure dynamical fidelity.

one can evolve in a physically realistic (and computationally efficient) way a system of strongly-interacting particles. In Section V we apply this algorithm to a system of self-assembling components designed to model the aggregation of protein complexes called chaperonins. We conclude in Section VI.

II. RESTORING ERGODICITY TO CONVENTIONAL MC CLUSTER ALGORITHMS

In this section we show that a simple modification of existing MC cluster algorithms [7, 9], can be used to restore ergodicity to simulations of strongly-attractive particles. Let us explain our scheme and nomenclature with reference to Figure 2. Here we consider in d dimensions a system of N particles endowed with a hard-core radius a , and a short-ranged, pairwise potential ϵ_{ij} . Shown is a typical cluster move (and its reverse) from state μ to state ν . We shall describe two particles as contiguous if they are separated by a distance less than or equal to the interaction range of the potential. We define a *physical cluster* (abbreviated simply to 'cluster') as a group of contiguous particles. We shall use an iterative linking

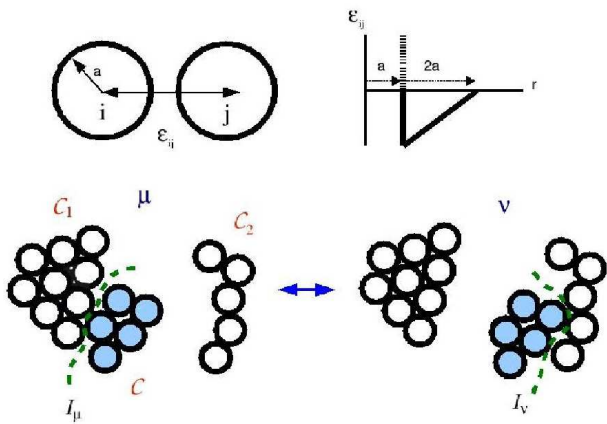


FIG. 2: An illustrative cluster move for our example system, hard core particles of radius a endowed with an attractive linear pair potential of range $2a$. We define a pseudocluster \mathcal{C} (blue particles; see text), and subject it to a rotation or a translation. Here a proposed translation moves \mathcal{C} from contact with cluster \mathcal{C}_1 in state μ to contact with cluster \mathcal{C}_2 in state ν . The interface between the pseudocluster and its environment in state α is labelled \mathcal{I}_α , and is defined by the set of all pairwise interactions between white and blue particles.

procedure, described below, to select a group of particles. This group can range in size from a single particle to any one cluster in the system. We shall call this group of particles a *pseudocluster*. In Figure 2 the pseudocluster \mathcal{C} is shown in blue. We perform on \mathcal{C} either a rigid-body rotation about an arbitrary axis through its centre of mass, or a translation in an arbitrary direction. In the figure, one such translation happens to bring the pseudocluster into contact with the cluster \mathcal{C}_2 .

The concept of detailed balance ensures that a system evolves towards equilibrium by requiring that the rates W for passing between any two states μ and ν satisfy

$$\rho(\mu)W(\mu \rightarrow \nu) = \rho(\nu)W(\nu \rightarrow \mu). \quad (1)$$

Here $\rho(\alpha) = Z^{-1}e^{-\beta H_\alpha}$ is the Boltzmann weight with respect to the system's Hamiltonian in state $\alpha \in \{\mu, \nu\}$, H_α ; $\beta \equiv 1/T$ is the reciprocal temperature (we define $k_B \equiv 1$); and Z is the partition function. The rates W in general depend on the fictitious reciprocal temperature β_f . Equation (1) ensures that detailed balance is respected *provided* that the distribution $Q(\beta_f)$ from which β_f is drawn is the same for both transitions $\mu \leftrightarrow \nu$.

The rate for passing between states is the product of the rates of proposing (generating) and of accepting such a move: $W(\mu \rightarrow \nu) = W_{\text{gen}}(\mu \rightarrow \nu)W_{\text{acc}}(\mu \rightarrow \nu)$. One can then determine the ratio of acceptance rates such that detailed balance (1) is respected:

$$\frac{W_{\text{acc}}(\mu \rightarrow \nu)}{W_{\text{acc}}(\nu \rightarrow \mu)} = \frac{\rho(\nu)W_{\text{gen}}(\nu \rightarrow \mu)}{\rho(\mu)W_{\text{gen}}(\mu \rightarrow \nu)}. \quad (2)$$

We evaluate the right hand side of this equation as follows. To define a pseudocluster \mathcal{C} we select from the

system a ‘seed’ particle i . We form links between i and all other particles j with probability

$$p(i, j) = \max\left(0, 1 - e^{\beta_f u_f(\epsilon_{ij})}\right). \quad (3)$$

Here $u_f(\epsilon_{ij})$ is a fictitious potential, and can be chosen for convenience. A simple choice is $u_f(\epsilon) = \epsilon \Theta(r_0 - r)$; $u_f(\epsilon) = \epsilon$ within some cutoff distance r_0 , and zero otherwise. This renders potentials of arbitrary range amenable to the iterative linking scheme described below.

From each linked particle j we form links with probability $p(j, j')$ to all particles j' not already linked to i . We iterate this procedure until no further links form. For a system with short-ranged interactions ϵ , or a system in which $u_f(\epsilon)$ is chosen to be short-ranged, each stage k of the iteration corresponds essentially to considering the k -th nearest neighbours of i .

Linking particles in the manner dictated by Equation (3) results in the pseudocluster \mathcal{C} (see Figure 2) being selected and moved with probability

$$W_{\text{gen}}(\mu \rightarrow \nu) = P_{\text{seed}}(\mu)P_{\text{build}}(\mathcal{C}; \mu)W_{\text{move}}(\mathcal{C}; \mu \rightarrow \nu). \quad (4)$$

Here $P_{\text{seed}}(\mu)$ accounts for the likelihood of choosing a seed particle in the pseudocluster \mathcal{C} . The factor $P_{\text{build}}(\mathcal{C}; \mu)$ returns the *a priori* probability of building the pseudocluster \mathcal{C} in microstate μ , given that the seed particle has been chosen. This depends on two factors:

$$P_{\text{build}}(\mathcal{C}; \mu) = \prod_{\mathcal{I}_\mu} [1 - p(i, j)] \prod_{\mathcal{R}} p(i, j). \quad (5)$$

The product over the interface \mathcal{I}_μ is the likelihood that no links are formed between \mathcal{C} and its environment in state μ . From (3), this product is equal to $e^{\beta_f U_\mu}$, where $U_\mu \equiv \sum_{\mathcal{I}_\mu} \min(0, u_f(\epsilon_{ij}))$ is the attractive part of the fictitious interfacial energy between the pseudocluster \mathcal{C} and its environment in state μ . The second factor in (5) is the probability of forming links between the constituent monomers of \mathcal{C} . In general there are many distinct realizations of links leading to the same chosen pseudocluster, and the product runs over one such realization \mathcal{R} . This piece will be canceled by the corresponding factor for the reverse move $\nu \rightarrow \mu$.

The third factor in (4), $W_{\text{move}}(\mathcal{C}; \mu \rightarrow \nu)$, is the rate for moving (translating and rotating) the pseudocluster \mathcal{C} , so that the system adopts microstate ν . Here we shall consider a uniform distribution of translations and rotations, in which case $W_{\text{move}}(\mathcal{C}; \mu \rightarrow \nu) = W_{\text{move}}(\mathcal{C}; \nu \rightarrow \mu)$.

Finally, we note that the internal cluster energies in states μ and ν are identical, and so the ratio of Boltzmann weights $\rho(\nu)/\rho(\mu)$ reduces to $e^{-\beta(E_\nu - E_\mu)}$, the exponential of the difference of the reduced interfacial energies between \mathcal{C} and its respective environments. Here $E_\alpha \equiv \sum_{\mathcal{I}_\alpha} \epsilon_{ij}$. The generation rate for the reverse move $W_{\text{gen}}(\nu \rightarrow \mu)$ differs from its counterpart for the forward move (4) only in the product over the interface in P_{build} , and the factor $P_{\text{seed}}(\nu)$.

Putting this collection of results together allows us to evaluate (2), the ratio of acceptance rates for moving between states μ and ν :

$$\frac{W_{\text{acc}}(\mu \rightarrow \nu)}{W_{\text{acc}}(\nu \rightarrow \mu)} = \frac{P_{\text{seed}}(\nu)}{P_{\text{seed}}(\mu)} e^{-\beta(E_\nu - E_\mu) + \beta_f(U_\nu - U_\mu)}. \quad (6)$$

Henceforth we shall choose our seed particle with uniform probability. Provided that the number of particles N does not change, $P_{\text{seed}}(\alpha) = 1/N$, independent of the state α . The ratio $P_{\text{seed}}(\nu)/P_{\text{seed}}(\mu)$ is then unity. For the move $\mu \rightarrow \nu$, we choose as the acceptance probability

$$p_{\text{acc}}(\mu \rightarrow \nu) = \min \{1, \exp(-\beta E_{\nu,\mu} + \beta_f U_{\nu,\mu})\}. \quad (7)$$

Here $E_{\nu,\mu} \equiv E_\nu - E_\mu$ and $U_{\nu,\mu} \equiv U_\nu - U_\mu$. Recall that E_α denotes the interfacial energy between pseudocluster \mathcal{C} and its environment in a given microstate, $E_\alpha \equiv \sum_{\mathcal{I}_\alpha} \epsilon_{ij}$; $U_\alpha \leq 0$ denotes the *attractive part* of the *fictitious* energy between \mathcal{C} and its environment, $U_\alpha \equiv \sum_{\mathcal{I}_\alpha} \min(0, u_f(\epsilon_{ij}))$.

Since one Monte Carlo step corresponds to a trial move of one particle, a move of n particles collectively represents an advance of n Monte Carlo steps; time should be updated accordingly.

In Section III we shall focus on the case where the interparticle potential is attractive $\epsilon_{ij} < 0$, and we shall set the fictitious potential $u_f(\epsilon_{ij})$ equal to the true potential ϵ_{ij} . In this case the procedure we have described is particularly straightforward to implement. Particles are linked according to a simple probability, $p(i, j) = 1 - e^{-\beta_f |\epsilon_{ij}|}$, and the ratio of acceptance rates is a simple function of the change in energy resulting from the move. For the move $\mu \rightarrow \nu$, the acceptance probability (7) reduces to

$$p_{\text{acc}}(\mu \rightarrow \nu) = \min \left(1, e^{(\beta_f - \beta)(E_\nu - E_\mu)} \right). \quad (8)$$

For infinite fictitious temperature, $\beta_f = 0$, the likelihood of forming links between the seed i and any other particle is zero, and so the algorithm executes single-particle moves with Metropolis acceptance probability $\min(1, e^{-\beta(E_\nu - E_\mu)})$. For a fictitious temperature equal to the true temperature, $\beta_f = \beta$, and for attractive interactions, the acceptance probability is unity, and the algorithm reduces to an off-lattice generalization [7] of the Swendsen-Wang cluster algorithm [9].

By drawing a fictitious reciprocal temperature in the range $\beta_f \in [0, \beta]$, we can interpolate between single-particle moves and rejection-free cluster moves. In the following section we demonstrate the advantage offered by generalizing the rejection-free cluster algorithm to one possessing a lower acceptance rate, but, crucially, an improved *proposal* rate. When applied to a tightly-bound aggregate of particles, the rejection-free scheme does not allow the construction of pseudoclusters smaller than the aggregate. Thus the aggregate cannot relax through moves in concert of its constituents. In other words, the *generation* rate for many transitions involving collective motion of tightly-bound particles is close to zero. By

contrast, varying β_f allows one to increase markedly the generation rates of these moves, at the affordable cost of reducing slightly their acceptance rates. As a result, one can choose from the aggregate pseudoclusters of arbitrary size, and thus propose collective internal relaxations in the presence of arbitrarily strong interactions. We refer to this procedure as cluster ‘cleaving’.

In the following section we demonstrate that the cleaving algorithm provides a simple way of restoring ergodicity to Monte Carlo simulations of strongly-interacting particles. In Section IV we introduce a virtual-move Monte Carlo cluster algorithm designed to evolve such systems in a dynamically realistic fashion.

III. AVOIDING KINETIC TRAPS ASSOCIATED WITH REJECTION-FREE MOVES

To illustrate the nature of the kinetic traps our cluster cleaving algorithm is designed to avoid, we present data from Monte Carlo simulations of a system of pairwise-interacting particles. The system we study is chosen to be difficult to simulate using only single-particle techniques and the rejection-free cluster algorithm, namely a collection of strongly-interacting particles. That said, our test system is a prototype of a dense, strongly-interacting aggregate; physical realizations include a colloidal gel bound by strong depletion interactions [20], and a dense aggregate of soot particles [21]. The strength of interaction need be only a few $k_B T$ before conventional MC single-particle or rejection-free cluster algorithms encounter unphysical kinetic traps. In our example we choose an interaction much stronger, to demonstrate that the cleaving algorithm can cope with arbitrarily strong interactions.

Our test system consists of 64 hard disks of diameter a in two dimensions, endowed with an attractive piecewise-linear pair potential of range $2.15a$. The contact energy rises linearly from $-50k_B T$ at $r = a$ to $-0.05k_B T$ at $r = 2.12a$, and is constant until $r = 2.15a$. Otherwise, it is zero. This system possesses a thermodynamically stable ground state corresponding to an hexagonal close-packed sheet. We measure time in units of Monte Carlo sweeps.

We can demonstrate the type of metastable structure that develops in the presence of the rejection-free cluster algorithm by ordering the system initially as a *square* lattice (with some positional disorder). Both the cleaving and the rejection-free cluster algorithms attempt to relax the system to its hexagonal close-packed ground state. We use a physically realistic maximum step size of about one particle radius. In Figure 3 we show a sequence of configurations obtained in this manner. On the left we show a sequence obtained using a mixture of single-particle moves and cluster moves in the the rejection-free limit, and on the right we show a sequence obtained using a mixture of single-particle moves and the cleaving algorithm. We find that relaxation is frustrated and

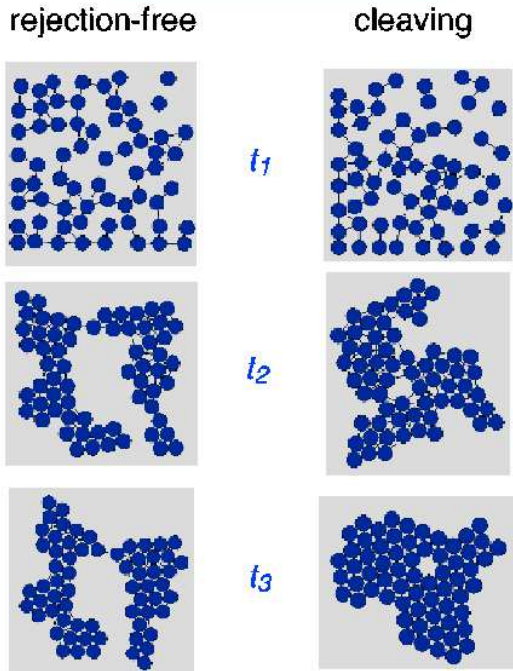


FIG. 3: Simulations of our test system (see text) at times $t_1 = 10^0$, $t_2 = 10^{5.2}$ and $t_3 = 10^{6.4}$, from top to bottom (see Figure 3). We show inter-particle interactions as lines joining particles. Left panels: rejection-free cluster algorithm, leading to a jammed configuration. Right panels: cleaving algorithm, which circumvents the unphysical kinetic traps associated with rarely testing strong inter-particle bonds. This leaves the system free to explore the physical kinetic traps associated with the rearrangement of a dense structure.

that ‘jammed’ structures persist for the single-particle moves in combination with rejection-free cluster moves. These jammed structures owe their existence to the following mechanism. First, radial potential energy gradients encourage neighbouring particles to aggregate into dense clumps separated by voids of lower density, a relaxation that can be accomplished readily by single-particle moves. Thereafter, because of the strength of the inter-particle contacts, the rejection-free cluster algorithm fails to propose moves of one clump relative to another. Since the structure does not readily relax in a single-particle fashion, the system finds itself in an unphysical kinetic trap. The unphysical nature of this trap results from a failure to test the potential energy *gradients* of strong inter-clump contacts.

The cleaving algorithm circumvents this trap. For sufficiently large T_f all contacts are tested. The algorithm may propose moves of one clump relative to another, and the system can relax via collective moves of its constituents. For a physically realistic step size, relaxation using even the cleaving algorithm is slow because of the *physical* kinetic traps associated with the rearrangement of a dense structure. Algorithms better suited to studying the equilibrium properties of dense structures [7, 22]

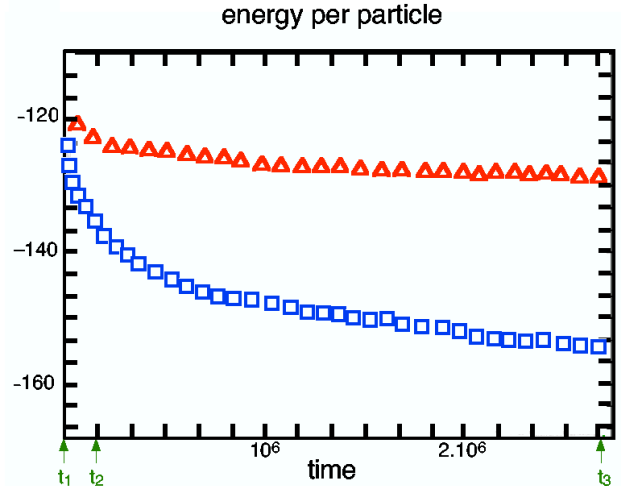


FIG. 4: Energy E as a function of time t for the rejection-free cluster algorithm plus single-particle moves (upper line, red) and the cleaving algorithm plus single-particle moves (lower line, blue); we show data averaged over 10 simulations for each case. Following the early-time single-particle-dominated relaxation, the standard cluster algorithm becomes ensnared by an unphysical kinetic trap, and the energy arrests. For sufficiently strong inter-particle interactions this arrest is indefinite. The cleaving algorithm circumvents this unphysical trap. The configurations shown in Figure 2 were taken at the times marked by the green arrows.

could then be employed.

In Figure 4 we show a quantitative measure of the difference between the two algorithms. We plot the energy of the system as a function of time for both the rejection-free cluster algorithm plus single-particle moves (upper line) and the cleaving algorithm plus single-particle moves (lower line). The early relaxation in the two cases is dominated by single-particle moves and is similar. At later times the cleaving algorithm’s ability to circumvent the unphysical kinetic traps which plague the rejection-free algorithm is evident. In the simulations shown we drew the fictitious reciprocal temperature from a uniform distribution, to emphasise that considerable time savings can be obtained even with no prior knowledge of the quantitative strength of the inter-particle attractions.

IV. A DYNAMIC MONTE CARLO ALGORITHM

Self-assembly is the process whereby interacting components organize spontaneously into thermodynamically stable patterns or aggregates. It is the means by which many biological structures form, from the protein packaging of viruses [17, 18] to the lipid membranes enclosing cells. The self-assembly of nanometer-scale objects constitutes an important branch of nanotechnology.

In studying self-assembly, it is important to identify the nature of the inter-component interactions that can lead to stable structures with the required symmetry. However, a full understanding of how assembly is effected requires a characterization of its dynamics. Binding that depends on the precise alignment of neighbouring components might ensure thermodynamic stability, but the time required for two bodies to collide in this manner could be prohibitively long. Similarly, very strong contacts contribute to the stability of equilibrium structures but could also transiently stabilize malformed aggregates, thereby impeding equilibration.

Brownian dynamics is perhaps the most natural kinetic model for several examples of biological self-assembly, given the relatively large sizes and small diffusivities of many proteins. However, component-component interactions take place on a timescale many orders of magnitude less than assembly of the overall structures. As aggregation proceeds, productive rearrangements increasingly require the concerted motion of many components. If the steric constraints of each body are to be preserved, the simulation time step must remain much smaller than the rate of such movement. Integrating equations of motion in this case is a very costly way to update the system.

While the cluster cleaving algorithm we have presented does not suffer from this problem, neither does it evolve a self-assembling system in a manner fully in accord with natural dynamics. The reason for this deficiency is that clusters are moved according to bond *energies*, not energy *gradients*. In the Appendix we show analytically that this scheme corresponds to an unrealistic dynamics, in which a particle's drift velocity is not simply proportional to the negative of the potential energy gradient it experiences.

In this section we shall introduce our central result, a dynamic cluster algorithm. This algorithm is designed to reproduce physical dynamics for interacting bodies, by moving them either individually or in concert according to individual bond energy gradients. We divide this section into two parts. In the first part we describe in detail the basic virtual-move scheme we shall consider. In the second part, we describe how a concatenation of such moves can be used to simulate a system of interacting particles, by moving all particles with equal frequency according to the potential energy gradients they experience. In this way we can effect a realistic evolution of a self-assembling system without explicit computation of forces.

A. A virtual-move Monte Carlo algorithm

Refer to Figure 5. Here we consider four particles, 0, 1, 2 and 3, endowed with an orientation-dependent interaction (particle orientation not shown). The system starts in state μ . As a result of their orientations and separations, particles 0 and 1 interact strongly, with energy $\epsilon_{01} = -\sigma_1$. Particles 1 and 2 interact very strongly, with energy $\epsilon_{12} = -\epsilon$. Particles 2 and 3 interact weakly, with

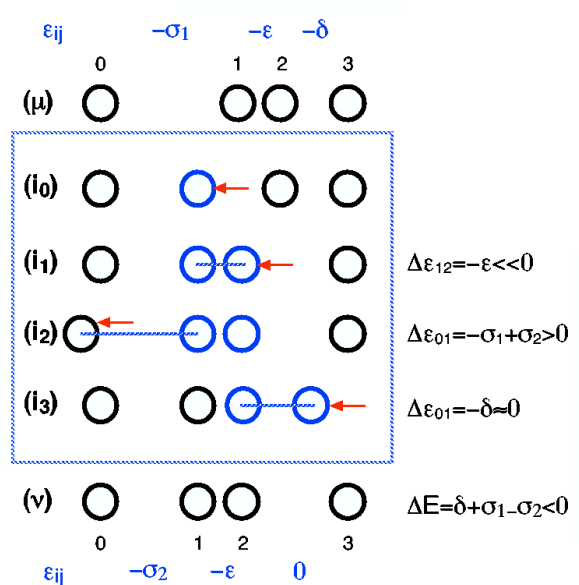


FIG. 5: An illustration of the virtual-move Monte Carlo algorithm. From starting state μ , the seed particle 1 executes a virtual move leftwards a distance Δ . The new state is intermediate state zero, \mathbf{i}_0 . Thereafter, we test in an iterative fashion (using Equation (9)) all interacting particles, via a series of virtual moves. Proposed bonds are shown as horizontal blue lines joining particles. In the example shown, the virtual move leading to intermediate state \mathbf{i}_1 is accepted, but virtual moves leading to states \mathbf{i}_2 and \mathbf{i}_3 are rejected. Intermediate state \mathbf{i}_1 is then proposed as the final state ν . This state is automatically accepted, provided no particle overlaps occur. Only particle 2 has moved in concert with particle 1. The large blue box indicates that evaluation of the Monte Carlo acceptance criterion is delayed until the final line of the figure.

energy $\epsilon_{23} = -\delta$. We imagine that if particles 0 and 1 approach each other a little more closely, their energy of interaction becomes slightly greater, $-\sigma_2$. We assume that the interaction between 1 and 2 is very short-ranged, and any increase in the separation of these particles causes this energy to be lost. We also imagine that the weak interaction $-\delta$ between 2 and 3 is lost if their separation increases slightly, but does not increase if their separation decreases. The energy hierarchy is $\epsilon \gg \sigma_2 > \sigma_1 \gg k_B T$, $\delta \leq k_B T$.

A ‘natural’ dynamics would see the dimer 12 attracted towards particle 0, in order to raise the binding energy 01 from σ_1 to σ_2 . As discussed previously, single-particle moves applied to particles 1 or 2 would likely be rejected, because most moves would break the bond between these particles. Since the energy ϵ is much greater than $k_B T$ and any other energy in the system, the acceptance rate for such a break would be very small. The rejection-free cluster move would likely link particles 0, 1 and 2, because both energies ϵ_{01} and ϵ_{12} are much greater than $k_B T$. No move of the dimer 12 relative to 0 would then be possible. The basic cleaving move we have discussed

would propose a collective move of 12 relative to 0, although not in a dynamically realistic fashion (see Appendix). To ensure dynamical fidelity, we propose the following algorithm.

Make a sequence of ‘virtual’ local particle moves, and accept these moves based on changes in *individual* bond energies. Only when all of these intermediate moves have been attempted is the change in total energy evaluated and the Metropolis acceptance criterion applied. In Figure 5, our proposed scheme unfolds as follows. We select at random a seed particle (particle 1), and assign to it a *virtual* move according to a *map*, which defines a random translation or rotation. We shall denote the state of particle i by $x_i = \{\mathbf{r}_i, \mathbf{S}_i\}$ (which encodes the position \mathbf{r}_i and orientation \mathbf{S}_i of the particle). We denote translations or rotations by the operation $x'_i = \mathcal{U}_{x_i} x_i$, \mathcal{U}_{x_i} being the *move map* in question. For translations, the map \mathcal{U}_{x_i} is independent of x_i . For rotations, we choose an arbitrary axis through the centre of mass of the seed particle; \mathcal{U}_{x_i} effects rotations about this axis.

In the example, the move map defines a leftward translation of magnitude Δ . We first apply this map to particle 1. The virtual move of 1 moves it closer to particle 0, and further from particle 2. The interaction 12 is lost, and the interaction 01 is increased slightly to $-\sigma_2$. We refer to this virtual state as *intermediate state zero*, or \mathbf{i}_0 . Note that in a standard Monte Carlo scheme a move to this state would almost certainly be rejected, because of the loss of the binding energy $-\epsilon$. However, during intermediate steps \mathbf{i}_n (shown boxed in Figure 5) we do not evaluate the Monte Carlo acceptance criterion. This evaluation is delayed until all intermediate steps have taken place.

Starting from state \mathbf{i}_0 we attempt a series of virtual moves of all particles in the same physical cluster as the seed particle, in order to test whether these particles link to (and so move in concert with) the seed particle. We form links with probability

$$p_{\text{link}}(i, j) = \max(0, 1 - \exp\{\beta E_c - \beta E_I\}). \quad (9)$$

Here

$$E_c \equiv \epsilon_{ij} (x'_i - x'_j) = \epsilon_{ij} (x_i - x_j) \quad (10)$$

is the energy of the bond ij following a *collective* virtual move of i and j . Because the map defines either a rigid-body rotation or a translation, the particles do not move relative to each other, giving rise to the second equality in Equation (10). The energy

$$E_I \equiv \epsilon_{ij} (x'_i - x_j) \quad (11)$$

is the bond energy following an individual virtual move of i , and no move of j . With probability $p_{\text{link}}(i, j)$ we move i and j in concert, according to the specified move map. With the complementary probability, we do not move j . This is the key difference from a standard single-particle MC scheme: here, if the move of particle i relative to j is rejected, i and j are instead moved in concert.

In our example, the linking procedure unfolds as follows. First we test particle 2 to see if a link forms with particle 1 (proposed links are shown as horizontal lines between particles). The energy of bond 12 following a move of 1 relative to 2 is 0. Now make a virtual move of 2 under the prescribed map (leftwards a step Δ). The bond energy following this move is $-\epsilon$, just as in the original state μ : 1 and 2 have moved in concert. Call this intermediate state \mathbf{i}_1 . The change in energy of the bond 12 ($E_c - E_I$) is shown in the right-hand column of Figure (5). Since $\epsilon \gg k_B T$, we see from Equation (9) that the link 12 forms with probability close to 1. Thus particle 2 becomes part of the chosen pseudocluster, and is moved in concert with particle 1. Intermediate state \mathbf{i}_1 now becomes our ‘current’ state.

Next we attempt to form a link between the seed particle 1 and the other particle with which it interacted in state μ , particle 0. In state \mathbf{i}_1 the bond 01 has energy $-\sigma_2$. After particle 0 is moved (virtually) under the map, leftwards by Δ (call this state \mathbf{i}_2), the bond energy 01 is $-\sigma_1 > -\sigma_2$. From Equation (9), no link is formed between 0 and 1. Thus particle 0 does not become part of the pseudocluster, and it is not moved in concert with particles 1 and 2. We reject the virtual move of 0 (state \mathbf{i}_2), and return to intermediate state \mathbf{i}_1 .

As before, we iterate the link-forming procedure. All particles interacting with particle 1 have now been tested. Since particle 2 was successfully linked to 1, we now test all particles, not currently in the pseudocluster, which interacted with particle 2 in the original state μ . Particle 3 qualifies. The link 23 in state \mathbf{i}_1 has no energy. After a leftwards virtual move of particle 3 (state \mathbf{i}_3), this energy becomes $-\delta$. Since $\delta \ll k_B T$, the link-forming probability (9) is small, $p(i, j) \approx \delta/k_B T \ll 1$. In our example shown the link 23 is not formed. Particle 3 is not assigned to the pseudocluster, and its virtual move is rejected. We return to state \mathbf{i}_1 .

Now, iteratively, all particles interacting with those interacting with the seed particle have been tested. Only a link with particle 2 was formed, and so only particles 1 and 2 move collectively. We now propose the intermediate state \mathbf{i}_1 as the final state ν , and evaluate the Monte Carlo acceptance factor.

The acceptance probability for this procedure is straightforwardly evaluated from Equations (2), (4), (5) and (9). We refer again to Figure 2 as an illustration of a general move from a state μ to a state ν . If we choose the seed particle uniformly from any in the system, giving $P_{\text{seed}}(\mu) = P_{\text{seed}}(\nu)$. As before, the probability of forming links between particles such that the blue cluster is the chosen pseudocluster is independent of the pseudocluster’s environment, and so cancels from Equation (2). The remaining quotient in the latter equation concerns the probability of *not* forming links between the pseudocluster and its environment in each state. Equation (2) reduces to

$$\frac{W_{\text{acc}}(\mu \rightarrow \nu)}{W_{\text{acc}}(\nu \rightarrow \mu)} = e^{-\beta(E_\nu - E_\mu)} \frac{\prod_{\nu \rightarrow \mu} [1 - p(i, j)]}{\prod_{\mu \rightarrow \nu} [1 - p(i, j)]}. \quad (12)$$

The first factor on the right-hand side of Equation (12) is the ratio of the Boltzmann weights of the two states. As before, the energy E_α is the interfacial energy between the cluster and its environment in state α . The second factor denotes the link-breaking probabilities. The product $\prod_{\mu \rightarrow \nu}$ runs over all links which must not be formed in order to move from state μ to state ν .

Next we must evaluate the link-breaking factors. Consider the move from state μ to state ν . Imagine an intermediate state in which the blue pseudocluster has been moved according to the prescribed map, from contact with \mathcal{C}_1 to contact with \mathcal{C}_2 . This is (formally) state ν . Next, imagine a proposed intermediate step in which one of the white particles j executes a virtual move under the same map. To test whether a link forms, we evaluate the interaction energy between the white particle in question and each relevant particle i in the pseudocluster before and after the virtual move of j . After the virtual move of j , the interaction between ij is, by definition, the energy of this bond in the initial state, μ , which we write as $\epsilon_{ij}^{(\mu)}$. If j does not move according to the map, meaning that i has moved relative to j , the interaction is, again by definition, $\epsilon_{ij}^{(\nu)}$. Hence the probability of *not* linking the white particle in question to the pseudocluster is, from Equation (9),

$$1 - p(i, j) = \min \left(1, e^{\beta \epsilon_{ij}^{(\mu)} - \beta \epsilon_{ij}^{(\nu)}} \right). \quad (13)$$

The product of all such unformed links gives us

$$\prod_{\mu \rightarrow \nu} [1 - p(i, j)] = \prod_{\langle ij \rangle} \min \left(1, e^{\beta \epsilon_{ij}^{(\mu)} - \beta \epsilon_{ij}^{(\nu)}} \right), \quad (14)$$

where $\langle ij \rangle$ denotes all blue-white pairs. The factor corresponding to (14) for the reverse move follows by interchanging the labels μ and ν . Hence we have

$$\begin{aligned} \frac{\prod_{\nu \rightarrow \mu} [1 - p(i, j)]}{\prod_{\mu \rightarrow \nu} [1 - p(i, j)]} &= \prod_{\langle ij \rangle} e^{\beta \epsilon_{ij}^{(\nu)} - \beta \epsilon_{ij}^{(\mu)}} \\ &\equiv e^{\beta(E_\nu - E_\mu)}. \end{aligned} \quad (15)$$

Inserting this result in Equation (12) cancels the Boltzmann factor, giving a right-hand side of unity. Thus moving particles which interact *prior* to their moves is a rejection-free process.

We must also consider particles which interact following their moves, but did not interact beforehand. We accept these new interactions with the usual Metropolis probability, $p_{\text{acc}} = \min(1, e^{-\beta E})$, with E being the bond energy following the move (the bond energy prior to the move is zero by definition). We consider here particles with attractive interactions and hard walls. In this case if particles interact but do not overlap we automatically accept their new configurations; if particles overlap we automatically reject the whole virtual-move sequence. The virtual-move Monte Carlo scheme is therefore *rejection-free*, provided that the proposed final state contains no particle overlaps.

B. Simulating large systems with VMMC

In order to evolve a system of particles in a realistic fashion, all particles must be updated with equal frequency. The procedure described in the previous subsection does not fulfil this requirement. If we choose a seed particle uniformly from anywhere in the system, those particles residing in large physical clusters will suffer positional updates more frequently than those in small clusters. To see this, consider a system of 100 particles segregated into a cluster of 99 particles and a monomer. We choose a seed particle uniformly, and obtain with a probability of 0.99 a particle in the large cluster. Starting from this seed, we execute the iterative virtual move scheme. If the cluster is well-formed it will likely move as a rigid body. The positions of the other 98 particles in the large cluster will then be updated with a high probability. If we continue this procedure, each particle in the large cluster will be moved many more times than the monomer. This is unphysical.

In order to move all particles with the same frequency, we proceed as follows. We assign to *each* particle $j \in \{1, 2, 3, \dots, N\}$ a move map, (j) . We shall denote by $x_\alpha^{(\beta)}$ the coordinates of particle α following application of move map (β) . We then select uniformly a seed particle, and define this particle to be have the lowest possible numerical rank, zero. From the seed, we recursively test particle-pairs to determine whether particles move individually, or in concert. If they move in concert, we assign to the particle with the greater numerical rank the move map of the particle with the lesser numerical rank.

Consider two particles i and j , with coordinates (positions \mathbf{r} and orientations \mathbf{S}) denoted by x_i and x_j . We assign to each particle a move map, denoted (i) and (j) respectively. These maps are either random translations, or rotations about the centre of the particle in question. We select a seed particle, i . We now wish to decide whether to move i and j individually or in concert. To this end, we evaluate the right-hand-side of Equation (9), where now

$$E_c = \epsilon_{ij} \left(x_i^{(\kappa)} - x_j^{(\kappa)} \right) = \epsilon_{ij} (x_i - x_j) \quad (16)$$

is the pair energy following a collective move of particles i and j under either map $\kappa \in \{i, j\}$ (their relative separations and orientations do not change), and

$$E_I = \epsilon_{ij} \left(x_i^{(i)} - x_j^{(j)} \right) \quad (17)$$

is the bond energy following simultaneous individual moves of particle i under map (i) and particle j under map (j) . With probability $p_{\text{link}}(i, j)$ [Equation (9)] we move particles i and j collectively, according to the map of the particle with the lower numerical rank. In this case that particle is i , because it was chosen as the seed particle. Both particles then move according to map (i) . With probability $1 - p_{\text{link}}(i, j)$ the particles move individually, according to their own maps. For a system of

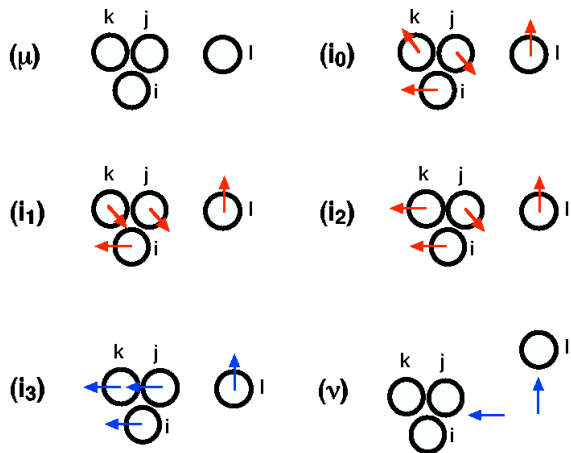


FIG. 6: An illustration of how to assign moves so that each particle moves exactly once per step, according to individual bond energy gradients (see text). An hierarchical system of conflict-resolution ensures that notional virtual moves (intermediate state \mathbf{i}_0) are changed according to individual bond energy gradients into the ‘real’ moves shown in intermediate state \mathbf{i}_3 . These moves are then executed simultaneously, taking the system from state μ to state ν .

arbitrary size, we repeat iteratively the above scheme until all move maps have been determined. To resolve opposing move-map assignments (‘tugs-of-war’) we use the following conflict-resolution algorithm.

1. Assign to all particles j a randomly-chosen move map (j).
2. Choose a seed particle, i , say. Assign to the seed a rank of zero. Particles with numerically low ranks will win tugs-of-war. Set the global ranking index to zero.
3. Look from i to all particles with which it interacts, $\{j\}$. To decide if i links to a given j , ask a) Is j unranked? b) Is the move map of particle i distinct from that of j ? If the answer to either question is yes, link i to j with probability $p_{\text{link}}(i, j)$. Note that this quantity depends on the current move map of each particle.
4. If i and j link, and if j is unranked or possesses a numerically larger rank than i , change the move map of j from (j) to (i), and assign to j the rank of i . Go to particle j , and proceed from step 3, with the replacement $j \rightarrow i$.
5. If i and j fail to link, and if j is unranked, add 1 to the global ranking index, and assign this value to j . Go to j , and proceed from 3, with the following caveat: attempt links from j only to *unranked* particles. If not, j will attempt to (redundantly) link back to i , effectively doubling the value of the interaction energy in the bond formation criterion

p_{link} . At step 3, use the replacement $j \rightarrow i$. If i and j fail to link and *both* possess ranks, do nothing.

6. If a particle i links to a neighbour j , and j ’s rank is numerically lower than i ’s rank, i adopts the move map and rank of j . Because i ’s move map has changed, return to step 3, and re-test links with all neighbours.
7. Steps 2 to 6 allocate moves to all particles in a given physical cluster. Next, choose a new seed particle uniformly from those particles in the system still unprocessed (necessarily in a different physical cluster), and proceed from step 2. Repeat step 6 until all clusters have been processed.

Now every particle in the system possesses a (final) move map. Execute all moves, and evaluate the Monte Carlo acceptance criterion. Since the VMMC algorithm has unit acceptance probability, this amounts to checking for particle overlaps. If any overlaps occur, replace all particles and proceed from stage 1. If no overlaps occur, accept the new configuration and increment Monte Carlo time by unity.

As a simple illustration of steps 1 to 6, consider Figure 6. Here we show four particles i, j, k and l , three of which (i, j and k) are bound together as a physical cluster. An example dynamic move could proceed as follows.

Start from microstate (μ). Assign move maps randomly to each particle [intermediate state (\mathbf{i}_0)]. Choose a seed particle, i . Suppose i fails to link to either j or k . Proceed to j . Let us say that j links to k , and so k adopts the move map of j (\mathbf{i}_1). Go to k . Because its move map has changed, we must attempt to link it to all of its neighbours. Suppose this time k links to i . Because i is the seed, and has the lowest numerical rank of all particles, k adopts the move map (and numerical rank) of i (\mathbf{i}_2). Since k has changed its move map, it must re-test its link with j . Let us say that this link forms. Then j adopts the move map and rank of k (\mathbf{i}_3).

The trimer has now been processed. Proceeding to the next particle, we see that l has no interactions and so moves according to its original map. All moves have been determined. Now we execute each move, passing to microstate (ν). No overlaps occur, and so this state is accepted.

In the above example we chose an awkward series of linkings and re-linkings within the trimer in order to demonstrate how such conflicts can be resolved. Typically, substantial moves from within a strongly-bound and well-formed cluster result in many or all particles in that cluster adopting the move map of the seed. Relatively little computational time is spent resolving conflicts of the nature described in the figure.

Detailed balance is unaffected by adopting the hierarchical conflict-resolution scheme we have described. Provided that the decision to move each pair of particles in concert or individually is made according to Equation (9), the algorithm satisfies detailed balance with an

acceptance rate of unity. We verified convergence to the Boltzmann distribution for the VMMC algorithm applied to the test case of a hard-particle attractive lattice gas in one dimension.

One can also incorporate a hydrodynamic scaling of cluster diffusion constants within the VMMC algorithm. Stokes' law states that a cluster of effective hydrodynamic radius R (the measure of the greatest extent of the moving cluster perpendicular to the direction of motion) possesses a translational diffusion constant $3D_t(R) = \Gamma R^{-1}$, and a rotational diffusion constant $8D_r(R) = \Gamma R^{-3}$, where $\Gamma \equiv k_B T (\pi \eta_w)^{-1}$; $\eta_w \approx 10^{-3}$ Pa s is the viscosity of water. Once all move maps have been determined, one can calculate for each collectively-moving group of particles their effective hydrodynamic radius R , where

$$R^2 = \langle |(\mathbf{r}_i - \langle \mathbf{r}_i \rangle) \times \hat{\mathbf{n}}|^2 \rangle. \quad (18)$$

The average $\langle \cdot \rangle$ is over the positions \mathbf{r}_i of all particles with identical move maps. The vector $\hat{\mathbf{n}}$ is either the direction of translation or the axis of rotation, as appropriate. Once R has been calculated, rescale proposed cluster translation steps by a factor R_0/R , (R_0 being the monomer radius), and proposed rotation angles by a factor $(R_0/R)^3$. Changes in bond energies between particles with different move maps are accepted with the Metropolis probability. This size- and shape-dependent drag becomes increasingly important when the system in question is composed of very polydisperse or anisotropic aggregates.

This completes our discussion of the the key result of this paper, the virtual-move Monte Carlo scheme. By forming links according to individual bond energies before *and after* a proposed move, we move particles (collectively or individually) according to individual bond energy gradients. The hierarchical conflict-resolution scheme described above ensures that the state of each particle is updated exactly once per move. This results in a dynamically realistic evolution of the system (see Appendix). Our scheme is computationally efficient, because moves are rejected only if particle overlaps occur. In addition, the calculation of energy differences bypasses the need for explicit computation of forces.

In the following section we apply this algorithm to a model of biological self-assembly.

V. APPLICATION TO SELF-ASSEMBLY

In the presence of ATP and magnesium ions, the heat shock protein (Hsp60) from the organism *Sulfolobus shibatae* self-assembles in two stages. First, monomers ('sub-units') of the protein assemble into 18-membered, nearly-spherical complexes ('units') of radius 17 nm. Next, units aggregate into extended structures often microns in scale. We refer to the 18-membered complexes as, interchangeably, 'units' or 'chaperonins'. Experiments with

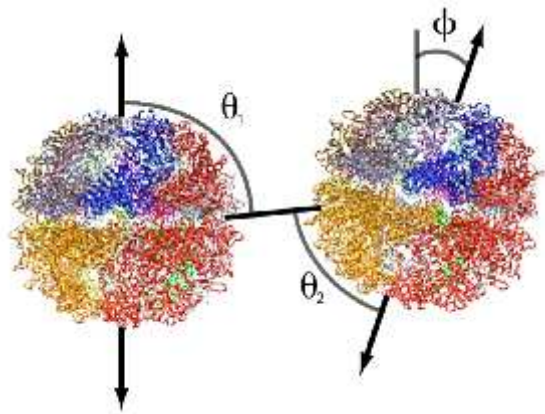


FIG. 7: Geometry for a schematic model of chaperonin self-assembly [11, 12, 13]. We use a short-ranged, anisotropic potential to mimic the tendency of chaperonins to bind either equator-to-equator or pole-to-pole. We show chaperonin structure determined by homology together with the angles relevant for our chosen interaction. The angle between orientation vectors is ϕ ; the angles between orientation vectors and the inter-unit separation vector are θ_1 and θ_2 .

the wild-type protein lead to two distinct types of chaperonin structures under subtly different external conditions: two-dimensional sheets with a high degree of hexagonal order, and quasi one-dimensional strings. We focus here on assembly into sheets, the control of which provides a means of engineering organic templates with a high degree of order, potentially useful for electronics devices. Free-floating sheets are also formed by the self-assembly of inorganic nanocrystals [27].

Computer models can help reveal the range of inter-chaperonin attraction strength and specificity required to effect large-scale sheet assembly. The detailed interactions between chaperonins are not known. Patterns of polar, nonpolar and charged amino acid side chains exposed by individual chaperonins do not immediately suggest specific regions where two units would strongly bind, nor do experimental results over a range of ionic strength clarify the physical nature of the binding interaction. It is clear, however, that forces between sheet-forming chaperonins favour equatorial contact. We can exploit this information when constructing a simple model of chaperonin self-assembly.

We build such a model by coarse-graining over the microscopic details of individual units (we consider units to be stable against dissociation into protein monomers). The simplest such approximation is to regard units as spheres without surface detail [25]. We mimic the effect of the microscopic unit-unit interactions by endowing spheres with a short-ranged, anisotropic pair potential designed to encourage mutual equatorial contact.

Figure 7 illustrates the geometry of our chosen potential. Each sphere has a polar orientation vector, shown as a double-headed arrow (we assume 'up-down' symmetry). We also assume azimuthal symmetry, so that

the pair potential does not change if spheres are rotated about their orientation vector. We choose the attraction to be strong if neighbouring orientation vectors are aligned ($\phi = 0, \pi$), and perpendicular to the inter-unit separation vector ($\theta_{1,2} = \pi/2, 3\pi/2$). Thus we allow only binding between complementary regions (equator-to-equator), and do not allow, for example, equator-to-pole binding. This reflects the near-perfect alignment observed between chaperonins in sheet-like assemblies, and also the notable absence of disordered aggregates [26].

Analytically, our chosen potential is

$$\epsilon(r) = -J_{\text{eq}} \Theta(2R + R_{\text{int}} - r) \hat{C}_1(\phi) \mathcal{C}_0(\theta_1) \mathcal{C}_0(\theta_2). \quad (19)$$

The step function Θ ensures that two spheres interact only when their surfaces are separated by a distance less than $R_{\text{int}} \equiv R_0/5$, R_0 being the unit radius. Here r is the distance between the centres of neighbouring chaperonins. We parameterize the angular interaction via the ‘cooperativity’ function $\mathcal{C}_\alpha(\psi) \equiv e^{-(\cos \psi - \alpha)^2/\sigma^2}$, which rewards an angle ψ if its cosine is within some tolerance (specified by a parameter σ) of the value α . The symmetrized cooperativity function $\hat{C}_\alpha(\psi) \equiv \mathcal{C}_\alpha(\psi) + \mathcal{C}_{-\alpha}(\psi)$ rewards values of $\cos \psi$ near $\pm\alpha$. The first angular factor in (19) encourages the alignment of neighbouring units; the second and third angular factors encourage mutual equatorial contact. We take $\sigma = 0.4$.

Here we demonstrate that the VMMC algorithm described in Section IV can identify several distinct mechanisms of sheet assembly, ranging from monomer addition to a single nucleus, to the binding and merging of separate sheet-like structures. We shall leave a detailed quantitative study of the rates of aggregation as a function of attraction parameters for elsewhere [28].

By assuming a chaperonin radius of $R_0 = 9$ nm, we obtain from Stokes’ law a translational diffusion constant for chaperonin monomers of $D_t(R_0) \approx 5 \times 10^{-11} \text{ m}^2\text{s}^{-1}$ (compare the self-diffusion coefficient of water, $D_{\text{H}_2\text{O}} \approx 5 \times 10^{-9} \text{ m}^2\text{s}^{-1}$). We draw monomer displacements Δ from a uniform distribution with extrema $\pm 1.28R_0$. From these data we calculate that our monomer displacement timescale corresponds to approximately 10^{-8} s. Thus a Monte Carlo step (1 VMMC step = 1 sweep) of 256 particles equates to roughly 10^{-5} s. We ran simulations for 10^6 to 10^7 MC steps, and so probe timescales of roughly 10 to 100 seconds. In experiments [11, 12, 13], large-scale assembly is observed on timescales of minutes to hours. Thus we expect our dynamic simulations to detect at least the onset of significant chaperonin self-assembly.

The relative rates of translation and rotation are fixed by imposing Stokes’ law for free monomers, namely $3D_t(R_0) = 8R_0^2 D_r(R_0)$. With a monomer diameter $2R_0 = 0.5$ units, we find that Stokes’ law is satisfied if we draw rotation angles from a uniform distribution with extrema $\pm 0.2\pi$.

We start from an initial state consisting of 256 monomers randomly dispersed and oriented in a 3d simulation box. We take periodic boundaries in each di-

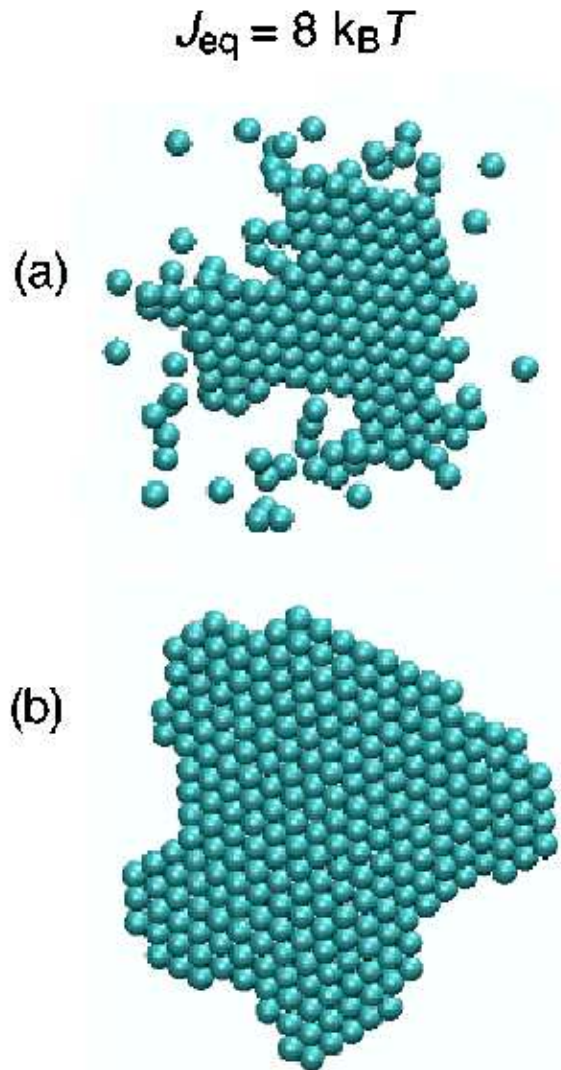


FIG. 8: Configurations at different times (**a**: $t = 3.572$; **b**: $t = 8.694$) for our schematic chaperonin system of spheres with sticky equators of strength $J_{\text{eq}} = 8k_B T$. For the concentration of units we consider, nucleation is rare, and self-assembly proceeds by the binding of monomers to a single sheet. The resulting structure is well-formed and defect-free.

mension. Units comprised about 1 % by volume of the simulation box, a lower concentration than is typically used in experiment. We then evolve the system according to the VMMC scheme. Times are quoted in millions of VMMC steps.

In Figure 8 we show configurations at different times for units with equatorial coupling $J_{\text{eq}} = 8k_B T$. Assembly proceeds, following a rare nucleation event, via the binding of monomers to a single sheet-like nucleus. The resulting structure is well-formed and nearly defect-free. The crossover from non-assembly to assembly is rather sharp: at the concentrations used, we observed no assembly within our simulation time at equatorial attrac-

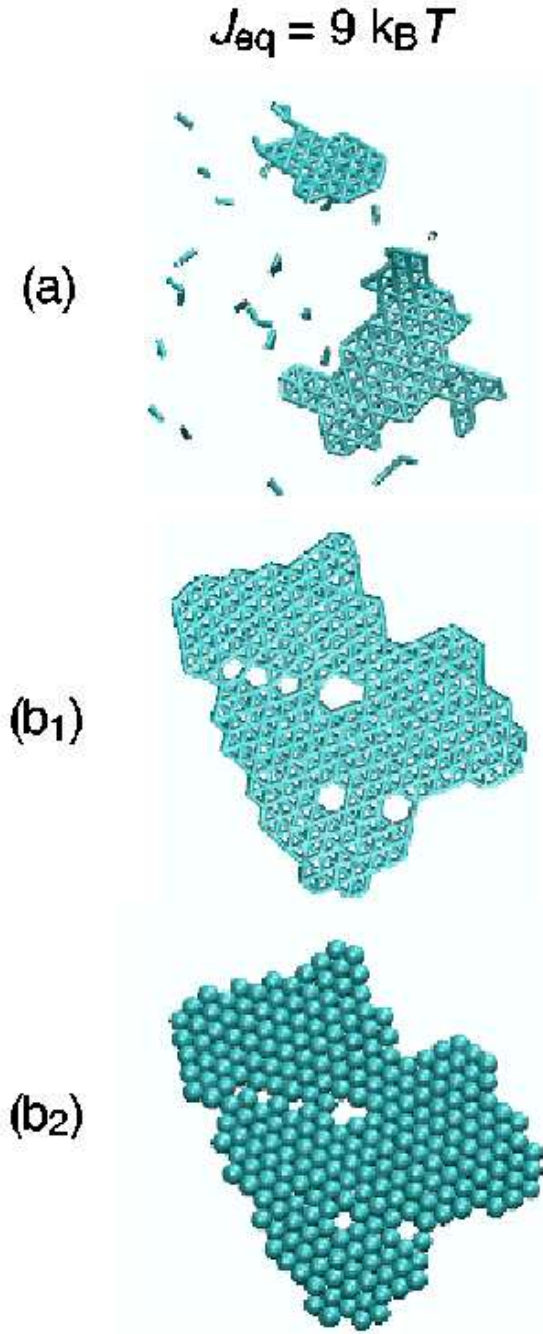


FIG. 9: Configurations at times $t = 0.18$ (a) and $t = 5.754$ (b₁, b₂) for our schematic chaperonin system with equatorial interaction strength $J_{\text{eq}} = 9 \text{ k}_B T$. Nucleation proves more rapid than at lower attraction strengths (Figure 8), and assembly involves the binding of two sheet-like structures. Here these structures collide awkwardly, leading to the defective sheet shown in panels b₁ (bond view) and b₂ (excluded-volume view).

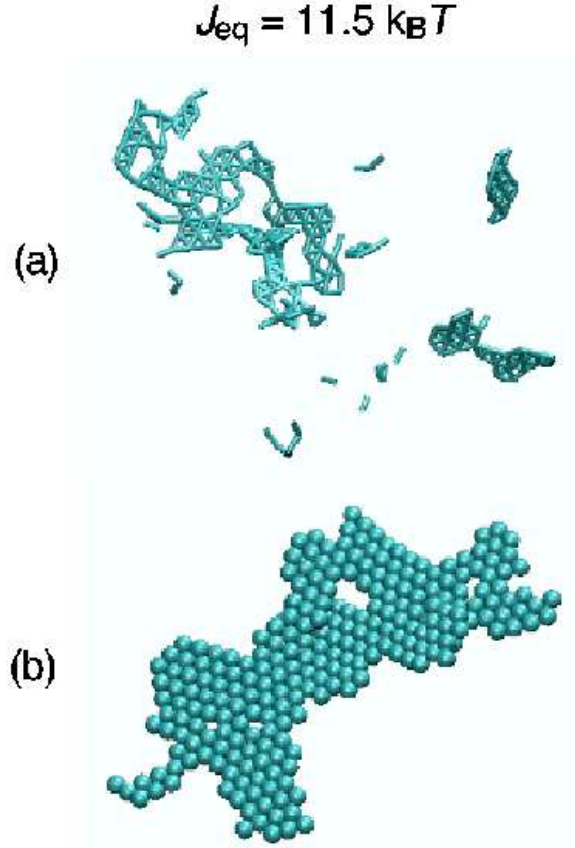


FIG. 10: Configurations at times $t = 0.034$ (a) and $t = 6.272$ (b) for our schematic chaperonin system with equatorial interaction strength $J_{\text{eq}} = 11.5 \text{ k}_B T$. Nucleation is so rapid that all intermediate structures are ill-formed (panel a). Collisions between these intermediates result in a structure trapped far from equilibrium (panel b).

tion strength $J_{\text{eq}} = 7.5 \text{ k}_B T$.

The change in assembly mechanism caused by increasing the unit-unit interaction strength is dramatic. At $J_{\text{eq}} = 9 \text{ k}_B T$ nucleation proves more rapid, and assembly proceeds via the binding of a few (typically 2 or 3) sheet-like structures, with monomers binding to all aggregates. Sheets tend to bind awkwardly, providing a defective template to which monomers bind. Defects do not anneal sufficiently rapidly, and the resulting structure is a kinetically trapped, malformed sheet. An example is shown in Figure 9.

At still higher attraction strengths (Figure 10), nucleation is so rapid that nuclei do not have time to relax into low energy sheet-like structures before they bind to other such ill-formed aggregates. In this regime assembly is frustrated kinetically.

These results indicate that the assembly mechanism for our schematic chaperonin model changes considerably with the unit-unit attraction strength. Because these interactions are angularly specific, particles must collide

equator-to-equator in order to bind. For insufficiently strong equatorial attractions, random collisions between monomers do not result in stable intermediates, and no assembly is seen. For sufficiently strong attractions, assembly proceeds via the binding of monomers to a single sheet-like nucleus. Aggregates grown in this way are typically well-formed and defect-free. Increasing unit-unit couplings beyond this point slows equilibration. Nucleation is promoted, and collisions between multiple sheet-like nuclei usually result in awkwardly-bound structures that relax only slowly. At very large attraction strengths nucleation is so rapid that the nuclei themselves are ill formed, leading to disordered aggregates.

VI. CONCLUSIONS

We have presented a virtual-move Monte Carlo cluster algorithm designed to permit the collective relaxation of particles possessing attractions of arbitrary strength, range and geometry, an important example being self-assembling particles endowed with strong, short-ranged and angularly specific ('patchy') attractions. By calculating pair energies before and after notional virtual moves, we deduce whether particles move individually or in concert. This scheme mimics the simultaneous updates of particle positions characteristic of molecular dynamics simulations. Its advantage over the latter lies in the fact that by computing energies before and after virtual moves, one bypasses the need to compute forces explicitly. We expect that this algorithm can be usefully applied to systems of self-assembling particles possessing a wide variety of attraction strengths, ranges and geometries.

A study is underway in which we compare Brownian dynamics with the VMMC algorithm, where each is used to effect the assembly of idealized protein capsomers into icosahedral virus capsids [18].

Acknowledgments

We thank Edward H. Feng, Matthew B. Francis, Michael Hagan, Robert L. Jack, Chad D. Paavola, Sander Pronk and Jonathan D. Trent for important discussions.

VII. APPENDIX: MONTE CARLO DYNAMICS

A. Single-particle moves

A Monte Carlo simulation consisting of a sequence of moves of individual particles can in many cases approximate natural dynamics. As a simple example, consider a collection of particles in one dimension in a potential $U(r)$. For sufficiently small step size Δ , a Metropolis Monte Carlo trajectory is equivalent to the behaviour described by a diffusive Fokker-Planck equation [4, 5].

Let us demonstrate this equivalence for a single particle with coordinate r in a potential $U(r)$. The master equation for the particle's motion is

$$\begin{aligned} \partial_t P(r; t) &= \int_{r'} P(r'; t) W(r' \rightarrow r) \\ &\quad - \int_{r'} P(r; t) W(r \rightarrow r'). \end{aligned} \quad (20)$$

Here $\int_{r'} \equiv \int_{r-\Delta}^{r+\Delta} dr'$, $P(r; t)$ is the probability of finding the particle at position r at time t , and $W(r \rightarrow r')$ is the rate for moving from position r to position r' . For a Metropolis acceptance rate the latter reads

$$W(r \rightarrow r') = W_0 W_{\text{gen}}(\delta r) \min\left(1, e^{-\beta[U(r')-U(r)]}\right). \quad (21)$$

The parameter W_0 is a reference frequency, and $W_{\text{gen}}(\delta r) = (2\Delta)^{-1}$ the *a priori* probability for choosing from a uniform distribution a step $\delta r \equiv r' - r$ in the range $[-\Delta, \Delta]$. The 'min' term encodes the Metropolis acceptance probability.

For a sufficiently small Δ one can expand Equation (20) in powers of $\hat{r} \equiv r' - r$. This is most easily done by changing the W notation from $W(r' \rightarrow r)$ to $W(r + \hat{r}; -\hat{r})$. The latter symbol means the rate for passing from configuration $r + \hat{r} (= r')$ to configuration $r + \hat{r} - \hat{r} = r$, and can be expanded in its first argument: $W(r + \hat{r}; -\hat{r}) = W(r; -\hat{r}) + \hat{r} \partial_r W(r; -\hat{r}) + \dots$. Likewise, $P(r', t) = P(r, t) + \hat{r} \partial_r P(r, t) + \dots$. To second order in ∂_r , Equation (20) reads

$$\partial_t P(r; t) \approx \partial_r (\langle \hat{r} \rangle P(r, t)) + \frac{1}{2} \partial_r^2 (\langle \hat{r}^2 \rangle P(r, t)), \quad (22)$$

with

$$\langle \hat{r}^k \rangle \equiv \int_{-\Delta}^{\Delta} d\hat{r} \hat{r}^k W(r; -\hat{r}). \quad (23)$$

The derivative-free term $\int_{r'} P(r, t) W(r; \hat{r}) - \int_{r'} P(r, t) W(r; -\hat{r})$ vanishes by symmetry. Equation (22) is a Fokker-Planck equation with drift velocity $v = -\langle \hat{r} \rangle$ and diffusion constant $D = \langle \hat{r}^2 \rangle$. Using Equation (21) we have to first order in \hat{r}

$$W(r; -\hat{r}) \approx \frac{W_0}{2\Delta} \min(1, 1 + \beta \hat{r} U'(r)). \quad (24)$$

We have assumed that $U'(r) \geq 0$ (which can be arranged by choosing the direction of increasing r appropriately), and also that $\hat{r}|U'(r)| \ll 1$. The latter condition is not true for a pathological potential such as (19), which possesses infinite gradients, but physically this is not a concern: the behaviour of a model with a 'regularized' potential (in which the step function is replaced by a sharp linear ramp) is similar to that of (19).

The integrals (23) can be evaluated in a piecewise fashion, with the minimum function in Equation (24) returning its first argument when $\hat{r} \geq 0$, and its second argument when $\hat{r} < 0$. To second order in Δ one can calculate

that the drift velocity is proportional to the potential gradient, $v = -(\beta/6)\Delta^2 W_0 \partial_r U(r)$, and that the diffusion constant is $D = \Delta^2 W_0/3$. This corresponds to Langevin dynamics satisfying an Einstein (fluctuation-dissipation) relation $-v/D = (\beta/2)\partial_r U(r)$. This result is straightforwardly generalized to many particles and higher dimensions. Note that normally v is independent of temperature T (not $\propto \beta$ as here), and $D \propto T$ (not independent of T). This can be arranged by making the fundamental attempt frequency W_0 proportional to T [5].

Thus Monte Carlo moves of single particles in a potential take place in a dynamically realistic way. As discussed in this paper, problems arise when such potentials become sufficiently strong and short-ranged that the basic step size must be made inconveniently small in order to prevent acceptance rates from vanishing. Long timescales result. The algorithms we have introduced remedy this problem. In the remainder of this Appendix we shall show that the cluster cleaving algorithm, which forms pseudoclusters by linking particle pairs according to their *energies*, corresponds only to an effective dynamics (a dynamics in which the drift velocity is not simply proportional to the potential gradient), and so should be strictly regarded only as a scheme for obtaining equilibrium averages. By contrast, the VMCM algorithm, which links particle pairs in a manner consistent with their potential energy *gradients*, corresponds to a realistic dynamics.

B. Cluster cleaving algorithm

Here we consider the dynamics of the cleaving algorithm, described in Section III. We use a fictitious potential equal to the true potential. Let us consider the separation vector x_{ij} between two particles i and j , which interact with an attractive pair potential $\epsilon_{ij}(x_{ij}) \leq 0$. Since the bond ij is independent of all others, the equation of motion of x_{ij} is all that is required for deducing the dynamical behaviour of the system.

For the cleaving algorithm, the master equation for the coordinate x_{ij} is

$$\begin{aligned} \partial_t P(x_{ij}; t) &= \int_{\hat{x}} P(x'_{ij}; t) W_c(x'_{ij} \rightarrow x_{ij}; \beta_f) \\ &\quad - \int_{\hat{x}} P(x_{ij}; t) W_c(x_{ij} \rightarrow x'_{ij}; \beta_f). \end{aligned} \quad (25)$$

Here $\int_{\hat{x}} \equiv \int Q(\beta_f) d\beta_f \int_{-\Delta}^{\Delta} d\hat{x}$, where $\hat{x} \equiv x'_{ij} - x_{ij}$; $P(x_{ij}; t)$ is the probability of observing a bond separation x_{ij} at time t ; and $W_c(x_{ij} \rightarrow x'_{ij}; \beta_f)$ is the rate at which the cleaving move changes the bond separation from x_{ij} to x'_{ij} .

The rate W_c at which the separation x_{ij} changes follows straightforwardly from Equations (3) and (8). We assume that either particle i or particle j is chosen as a seed, and displaced by the vector \hat{x} . Then the bond separation x_{ij} changes if 1) *no* link is proposed between i and

j , and 2) the Monte Carlo acceptance probability is satisfied. Condition 1) occurs according to Equation (3) with probability $\min(1, \exp\{\beta_f \epsilon_{ij}(x_{ij})\}) = \exp\{\beta_f \epsilon_{ij}(x_{ij})\}$. Criterion 2) is satisfied with a likelihood equal to the right-hand side of Equation (8). Hence

$$\begin{aligned} W_c(x_{ij} \rightarrow x'_{ij}) &= W_0 \exp\{\beta_f \epsilon_{ij}(x_{ij})\} \\ &\quad \times \min\left(1, e^{-(\beta - \beta_f)[\epsilon_{ij}(x'_{ij}) - \epsilon_{ij}(x_{ij})]}\right). \end{aligned} \quad (26)$$

Once again, W_0 is a reference frequency, and again we can expand the master equation (25) to second order in the small displacement Δ . We obtain the Fokker-Planck equation

$$\begin{aligned} \partial_t P(x_{ij}; t) &\approx -\partial_{x_{ij}}(v_{\text{eff}} P(x_{ij}; t)) \\ &\quad + \frac{1}{2} \partial_{x_{ij}}^2 (D \partial_{x_{ij}} P(x_{ij}; t)), \end{aligned} \quad (27)$$

with effective drift velocity

$$v_{\text{eff}} = v - \frac{1}{2} \partial_{x_{ij}} D. \quad (28)$$

The ‘bare’ drift velocity v is

$$v = -\frac{\Delta^2}{6} \hat{W} \cdot (\beta - \beta_f) \partial_{x_{ij}} \epsilon_{ij}(x_{ij}), \quad (29)$$

and the diffusion constant is

$$D = \frac{\Delta^2}{3} \hat{W}. \quad (30)$$

Here we have defined the position-dependent rate

$$\hat{W} = W_0 \int Q(\beta_f) d\beta_f e^{\beta_f \epsilon_{ij}(x_{ij})}, \quad (31)$$

which contains an integral over β_f (this integral acts on any β_f -dependent factors to its right). By virtue of the position-dependence of (31), the effective drift velocity is not simply proportional to the negative of the potential gradient. Instead, it is biased by a term depending on the exponent of the local bond energy:

$$v_{\text{eff}} = -\frac{\Delta^2}{6} W_0 \beta \partial_{x_{ij}} \epsilon_{ij}(x_{ij}) \int Q(\beta_f) d\beta_f e^{\beta_f \epsilon_{ij}(x_{ij})}. \quad (32)$$

This is unphysical. The cleaving algorithm evolves the system according only to an approximation of true Langevin dynamics: a particle’s drift velocity is not simply proportional to the potential gradient it experiences, nor is the diffusion constant (30) independent of position. Only in the (undesirable) limit of single-particle moves, $Q(\beta_f) = \delta(\beta_f)$, is physical dynamics restored. Note also that in the conventional rejection-free limit, $Q(\beta_f) = \delta(\beta_f - \beta)$, drift and diffusion are both suppressed by a factor $e^{-\beta|\epsilon(x)|}$, demonstrating that in the limit of strong attractions little motion is possible.

The root of these difficulties is the fact that pseudoclusters are built according to pair energies, and not energy gradients. However, drift and diffusion still satisfy the required Einstein relation for evolution to equilibrium,

$$-\frac{v_{\text{eff}}}{D} = \frac{\beta}{2} \partial_{x_{ij}} \epsilon_{ij}(x_{ij}). \quad (33)$$

C. VMMC algorithm

Next we turn to VMMC algorithm described in Section IV. With similar notation to before, the master equation for the separation x_{ij} between particles i and j is

$$\begin{aligned} \partial_t P(x_{ij}; t) &= \int_{\hat{x}} P(x'_{ij}; t) W_v(x'_{ij} \rightarrow x_{ij}) \\ &- \int_{\hat{x}} P(x_{ij}; t) W_v(x_{ij} \rightarrow x'_{ij}), \end{aligned} \quad (34)$$

where $\int_{\hat{x}} \equiv \int_{-\Delta}^{\Delta} d\hat{x}$. The rate W_v (the subscript stands for ‘virtual’) at which the separation x_{ij} changes follows straightforwardly from Equation (9). We assume that the combined virtual displacements of particles i and j under their respective move maps results in a change in the bond separation x_{ij} by \hat{x} . This change is accepted if 1) *no link* is proposed between i and j , and 2) the Monte Carlo acceptance probability is satisfied. Condition 1) occurs according to Equation (9) with probability

$$p_{\text{no link}}(ij) = \min(1, \exp\{\beta\epsilon_{ij}(x_{ij}) - \beta\epsilon_{ij}(x'_{ij})\}). \quad (35)$$

Condition 2) is automatically satisfied, provided that no particle overlaps occur. Thus

$$W_v(x_{ij} \rightarrow x'_{ij}) = W_0 p_{\text{no link}}(ij), \quad (36)$$

with $p_{\text{no link}}(ij)$ given by Equation (35).

An expansion of Equation (34) in powers of Δ yields a Fokker-Planck equation with a physically realistic drift velocity

$$v = -\frac{\Delta^2}{6} W_0 \beta \partial_{x_{ij}} \epsilon_{ij}(x_{ij}), \quad (37)$$

and a constant diffusion parameter

$$D = \frac{\Delta^2}{3} W_0. \quad (38)$$

The drift velocity is now proportional to the negative of the potential gradient. Provided that all particles in the system are updated with identical frequency (as described in Subsection IV B), the VMMC scheme corresponds to a realistic dynamics.

-
- [1] V.I. Manoussouhakis and M.W. Deem, J. Chem. Phys. **110**, 2753 (1999).
 - [2] O. Narayan and A. P. Young, Phys. Rev. E **64**, 021104 (2001).
 - [3] D. Frenkel and B. Smit, Understanding Molecular Simulation (second edition), Academic Press (2002).
 - [4] K. Kikuchi, M. Yoshida, T. Maekawa and H. Watanabe, Chem. Phys. Lett. **185** 335 (1991).
 - [5] G. Tiana, L. Sutto and R.A. Broglia, q-bio.0T/0606038 (2006).
 - [6] L. Berthier and W. Kob, cond-mat/0610235 (2006).
 - [7] J. Liu et al. Phys. Rev. E **71**, 066701, (2005); J. Liu and E. Luijten, Phys. Rev. Lett. **92** 035504, (2004).
 - [8] G. Orkoulas and A.Z. Panagiotopoulos, Fluid Phase Equilibria **93** 223 (1993); J. Chem. Phys. **101**, 1452, (1994).
 - [9] R.H. Swendsen and J.-S. Wang, Phys. Rev. Lett. **58** 86 (1987).
 - [10] K. Binder, Applications of the Monte Carlo Method in Condensed Matter Physics, Springer, Berlin (1984).
 - [11] R.A. McMillan, C.D. Paavola, J. Howard, S.L. Chan, N.J. Zaluzec and J.D. Trent, Nature Materials **1**, 247 (2002).
 - [12] J.D. Trent, H.K. Kagawa, T. Yaoi, E. Olle, and N.J. Zaluzec, Proc. Natl. Acad. Sci. USA **94**, 5383 (1997).
 - [13] M.J. Ellis M, S. Knapp, P.J.B. Koeck, Z. Fakoor-Biniaz, R. Ladenstein and H. Hebert, J. Struct. Biol. **123**, 30 (1998).
 - [14] M.A. Horsch, Z. Zhang and S.C. Glotzer, Phys. Rev. Lett. **95**, 056105 (2005).
 - [15] Z. Zhang, M.A. Horsch, M.H. Lamm and S.C. Glotzer, Nano Letters **3** (10), 1341 (2003).
 - [16] Z. Zhang and S.C. Glotzer, Nano Letters **4** (8), 1407, (2004).
 - [17] D.C. Rapaport, Phys. Rev. E. **70**, 051905 (2004)
 - [18] M.F. Hagan and D. Chandler, Biophys. J. **91**, 42 (2006).
 - [19] F. Wang and D.P. Landau, Phys. Rev. Lett. **86**, 2050 (2001).
 - [20] M. H. Lee and E. M. Furst, Phys. Rev. E **74** 031401 (2006).
 - [21] C. M. Sorensen, W. B. Hageman, T. J. Rush, H. Huang and C. Oh, Phys. Rev. Lett. **80** 1782 (1998).
 - [22] C. Mak, J. Chem. Phys. **122** 21, 214110 (2005).
 - [23] Wilber, A.M., et al. pre-print cond-mat/0606634 (2006).
 - [24] Z.-L. Zhang, A.S. Keys, T. Chen and S.C. Glotzer, Langmuir **21**, 25:11547 (2005).
 - [25] J. Harte, Consider a spherical cow. University Science Books (1988).
 - [26] C.D. Paavola, S.L. Chan, Y. Li, K.M. Mazzarella, R.A. McMillan and J.D. Trent, Nanotechnology **17**, 1171 (2006).
 - [27] Z. Tang, Z. Zhang, Y. Wang, S.C. Glotzer and N.A. Kotov, Science **314** 5797, 274 (2006).
 - [28] In particular, we ignore here the shape-dependent hydrodynamic damping of rotations and translations described in Section IV. Such an approximation affects aggregation rates, and is essential for a detailed quantitative study, but does not markedly change the mechanisms of assembly presented here.